

---

## Physics-Guided Multi-Attribute Petrophysical Inversion for Quantifying Acoustic Impedance and Porosity in the F3 Reservoir

Fadhur Rahman<sup>1\*</sup>, Abdul Haris<sup>1</sup>, Dwandari Ralanarko<sup>2</sup>, Humbang Purba<sup>2</sup>, Wrahaspati Rulandoko<sup>2</sup>, Praditio Riyadi<sup>3</sup>, Muhammad Nafian<sup>3</sup>, Muhammad Fahmi<sup>4</sup>

<sup>1</sup>Department of Physics, Universitas Indonesia, Indonesia.

<sup>2</sup>PHE OSES, RDTX Building, Indonesia.

<sup>3</sup>Department of Physics, Universitas Islam Negeri Syarif Hidayatullah Jakarta, Indonesia.

<sup>4</sup>Department of Physics, Faculty of Science and Mathematics, Diponegoro University, Indonesia

\*[fadhrhman1911@gmail.com](mailto:fadhrhman1911@gmail.com)

---

Submitted: October; Revised: November; Approved: December; Available Online: December

---

**Abstract.** This study presents a physics-guided multi-attribute inversion (PG-MAI) method to estimate acoustic impedance and porosity from post-stack seismic data using Bayesian Ridge Regression. The workflow integrates ten seismic attributes—including amplitude, frequency, and geometric features—into a regularized linear regression model. The physics-guided aspect is realized through the application of rock physics principles during data conditioning and interpretation, ensuring that the predictions remain physically and geologically meaningful. The Bayesian formulation introduces prior distributions over model coefficients to prevent overfitting and to quantify uncertainty, enhancing model robustness. Applied to the F3 Block in the Dutch North Sea, the inversion workflow involves temporal upsampling, attribute extraction, and calibration using two well logs. Results show strong spatial continuity and geological consistency, with high correlation (>0.90) between predicted and measured log values at both wells. Low-impedance and high-porosity zones align with deltaic sands and lobate geometries, indicating effective capture of facies heterogeneity. This approach demonstrates its value for reservoir characterization in complex siliciclastic settings.

**Keywords:** Acoustic Impedance, Physics Guided, Petrophysics, Inversion, Geocomputation

**DOI :** [10.15408/fiziya.v8i1.47182](https://doi.org/10.15408/fiziya.v8i1.47182)

### INTRODUCTION

Mapping subsurface rock properties is a fundamental task in geoscientific interpretation, particularly for delineating reservoirs with favorable porosity and impedance characteristics. These physical properties act as proxies for identifying lithological boundaries, fluid-bearing formations, and subsurface mechanical behavior under stress regimes [1]. Among them, acoustic impedance (AI) and porosity are critical for decoding rock fabric and assessing reservoir quality. However, direct measurements of these properties are limited to well

©2022 The Author (s) This is an Open-access article under CC-BY-SA license  
(<https://creativecommons.org/licenses/by-sa/4.0/>)

Al-Fiziya: Journal of Materials Science, Geophysics,  
Instrumentation and Theoretical Physics  
P-ISSN: 2621-0215, E-ISSN: 2621-489X

locations, which are typically sparse and unevenly distributed. This presents a significant challenge in capturing lateral variability and geological continuity. Moreover, estimating porosity from seismic data is inherently ill-posed due to issues such as non-uniqueness, limited vertical resolution, and sensitivity to noise. These limitations hinder the reliability of inversion results when extended away from well control. Therefore, there is a need for inversion frameworks that not only integrate multiple seismic attributes but also incorporate physical constraints to improve the accuracy and geological validity of predicted properties across the seismic volume.

To overcome the spatial limitations of well data, geophysicists utilize seismic data, which provide continuous lateral coverage and are sensitive to contrasts in elastic properties. Seismic inversion is employed to estimate quantitative rock properties, translating reflectivity information into acoustic impedance and porosity models. This is particularly critical in areas with limited borehole control, as it enables the extrapolation of petrophysical properties across the seismic volume. In post-stack seismic inversion—where offset-dependent amplitude variations (AVO) are absent—the inversion is constrained to single-trace reflectivity, reducing sensitivity to lithological changes [2]. Compared to pre-stack methods, post-stack inversion lacks angular information that can help differentiate fluid effects and rock stiffness, making it more susceptible to non-uniqueness and limited vertical resolution. Consequently, the inversion process must incorporate additional constraints, such as seismic attributes, to improve the robustness of predictions. Attributes such as amplitude envelope, instantaneous frequency, and geometric curvature provide auxiliary information related to energy distribution, stratigraphic variation, and structural patterns, thereby enhancing the geological interpretability of the inverted models. In this context, Bayesian inversion frameworks are particularly valuable, as they account for uncertainty and regularize solutions in the presence of noise and data limitations.

To compensate for such limitations, multi-attribute inversion techniques have been developed to exploit additional features derived from seismic traces, such as envelope, RMS energy, instantaneous phase, and signal curvature, which are physically meaningful and sensitive to lithological and stratigraphic variations [3]. In this study, ten seismic attributes were extracted per trace: original amplitude, amplitude gradient, Hilbert envelope, envelope derivative, RMS energy, Gaussian-filtered amplitude, relative impedance (log ratio), instantaneous phase, second-order curvature, and smoothed amplitude via medium-scale Gaussian filtering. The selection was guided by prior geophysical studies and preliminary correlation analysis with well log data, emphasizing both physical interpretability and statistical relevance. Redundancy among attributes was assessed using pairwise correlation metrics to minimize multicollinearity and ensure complementary information content. These features capture a broad spectrum of seismic responses, including reflectivity contrasts, spectral content, and geometric deformation. For example, RMS energy and envelope attributes enhance detection of high-energy facies, while curvature and amplitude gradient highlight structural discontinuities and subtle stratigraphic features. Collectively, their integration improves the inversion's ability to resolve facies transitions and predict rock properties with greater accuracy in complex geological settings.

A structured and transparent modeling approach is essential to mitigate overfitting and ensure geological plausibility in inversion results. Bayesian Ridge Regression (BRR) provides a mathematically principled solution by introducing prior distributions over model parameters, enabling an automatic trade-off between data fidelity and regularization [4]. In this study, we

adopt BRR as the core of the physics-guided multi-attribute inversion (PG-MAI) framework due to its closed-form solution, robustness to multicollinearity, and inherent ability to quantify predictive uncertainty. Compared to alternatives like Lasso, ElasticNet, or Support Vector Regression, BRR avoids the need for extensive grid-based hyperparameter tuning and offers probabilistic estimates that are particularly valuable in data-limited settings. Although the regularization parameters in BRR are inferred rather than manually set, cross-validation was still employed to ensure model generalization. The integration of physically interpretable attributes with BRR facilitates an explainable and reproducible inversion process, while the posterior covariance estimates provide insight into model confidence—an important advantage for reservoir characterization in geologically complex environments.

This investigation focuses on the F3 Block, a marine hydrocarbon reservoir located in the Dutch offshore sector of the North Sea. The area lies within a deltaic siliciclastic regime characterized by interbedded sandstone and shale formations that produce laterally heterogeneous seismic responses [5]. Situated in the southern part of the North Sea Basin and forming a subunit of the tectonically active West Netherlands Basin, the F3 Block presents stratigraphic complexity due to sedimentation spanning from the Jurassic to the Lower Cretaceous. The primary reservoir units belong to the Vlieland Sandstone, deposited in marginal marine to deltaic environments influenced by relative sea-level variations. These variations have generated vertically stacked parasequences and lateral facies transitions, which challenge conventional inversion methods due to impedance ambiguities and limited well control. The reservoir is seismically expressed through discontinuous reflectors, lobate geometries, and amplitude dimming in shale-dominated intervals—conditions that justify the application of a multi-attribute inversion approach. PG-MAI is particularly suitable for this setting because it integrates physical constraints with auxiliary attributes to better resolve the subtle impedance contrasts and stratigraphic heterogeneity inherent in the F3 system [6]. In deeper sections, Jurassic to lowermost Cretaceous (Hettangian–Berriasian) intervals record active rifting and paleogeographic compartmentalization, further complicating the seismic image and necessitating advanced inversion strategies [7].

Porosity values in the F3 Block have been reported to exceed 30% in clean sand layers, underscoring its strong reservoir potential [8]. Acoustic impedance in the same field typically ranges between  $2.5 \times 10^6$  and  $6.2 \times 10^6$  kg/m<sup>3</sup>·m/s, consistent with unconsolidated, shallow marine siliciclastics [9]. These well-documented properties establish a reliable baseline for evaluating inversion methodologies in a geologically complex setting. Building on this, the present study applies a physics-guided multi-attribute inversion (PG-MAI) framework to generate spatially continuous and geologically coherent estimates of porosity and acoustic impedance from post-stack seismic data. By leveraging well-log calibration and physically interpretable seismic attributes, the method seeks to improve prediction accuracy beyond traditional linear inversion. We hypothesize that integrating domain knowledge with probabilistic regularization will enhance the resolution and geological validity of inverted properties, particularly in deltaic settings with facies variability and limited angular information.

## RESEARCH METHODS

## Multi-Attribute Seismic Feature Analysis

Seismic attributes are mathematical transformations applied to seismic signals to extract diagnostic information about the subsurface. These transformations enhance measurable features such as amplitude, phase, and frequency, which are critical for identifying lithological variations and potential fluid zones [3]. In this study, the selected attributes were guided by a combination of rock physics correlations, prior literature, and exploratory data analysis, ensuring both physical relevance and predictive utility. For instance, the Hilbert envelope and RMS energy are sensitive to lithofacies and reflectivity strength, while curvature attributes highlight stratigraphic discontinuities and structural edges. Relative impedance aids in approximating lithological contrasts, and instantaneous phase captures waveform continuity. The integration of these attributes provides a richer input space than using amplitude alone, enabling improved prediction of reservoir properties when benchmarked against single-attribute inversions. Chopra and Marfurt emphasized that such multi-attribute frameworks are particularly valuable for stratigraphic and structural interpretation, offering enhanced resolution and geological context [10].

In this study, ten seismic attributes were utilized: original amplitude  $A(t)$ , amplitude gradient  $dA/dt$ , Hilbert envelope  $|H(t)|$ , envelope derivative  $d|H(t)|/dt$ , RMS energy, Gaussian-smoothed amplitude, relative impedance  $\log(|A(t)/A(t-1)|)$ , instantaneous phase, second-order curvature, and bandpass filtered amplitude.

The analytic signal formulation can be expressed as:

$$H(t) = A(t) + i\hat{A}(t) \quad (1)$$

Equation (1) defines the analytic signal,  $H(t)$ , as a complex-valued representation of a real seismic trace. In this expression,  $A(t)$  denotes the real-valued amplitude of the seismic signal at time  $t$ , which is the conventional output of seismic acquisition and processing [11]. To synthesize a complex seismic trace that encapsulates the signal's hidden structure, the Hilbert transform is unleashed upon the original amplitude function  $A(t)$ , producing its quadrature counterpart  $\hat{A}(t)$  a mathematically conjured imaginary signal that stands in perfect orthogonal contrast to its real twin. Functioning as a spectral phase-rotator, this transform re-phases every constituent frequency by 90 degrees, twisting the signal just enough to extract its elusive instantaneous attributes from the mathematical shadow

The imaginary unit  $i$ , where  $i^2 = -1$ , is introduced to form the complex component of the signal. By combining the original amplitude  $A(t)$  with its Hilbert-transformed counterpart  $i\hat{A}(t)$ , the analytic signal  $H(t)$  encodes both amplitude and phase information in a single expression. This formulation enables the computation of instantaneous seismic attributes such as envelope (the magnitude of  $H(t)$ ), instantaneous phase (the angle of  $H(t)$ ), and instantaneous frequency.

The analytic signal is fundamental in seismic attribute analysis, as it allows for more detailed interpretation of subsurface features through the lens of amplitude and phase variability. It is particularly valuable for detecting subtle stratigraphic changes, delineating thin beds, and characterizing fluid-sensitive responses.

$$|H(t)| = \sqrt{A(t)^2 + \hat{A}(t)^2} \quad (2)$$

Equation (2) defines the instantaneous amplitude or envelope of a seismic signal, denoted as

$|H(t)|$ . This expression is derived directly from the analytic signal  $H(t)$ , which was introduced in Equation (1) as  $H(t) = A(t) + i\hat{A}(t)$ . In the context of complex numbers, the magnitude (or modulus) of a complex signal  $z = x + iy$  is defined as  $|z| = \sqrt{x^2 + y^2}$ . Applying this to the analytic signal, where  $A(t)$  is the real part and  $\hat{A}(t)$  is the imaginary part, yields Equation (2)

The RMS amplitude over a temporal window is calculated to capture average energy content [12]:

$$RMS(t) = \sqrt{\frac{1}{\omega} \sum_{i=t-\frac{\omega}{2}}^{t+\frac{\omega}{2}} A(i)^2} \quad (3)$$

Equation (3) defines the Root Mean Square (RMS) amplitude of a seismic trace centered at time  $t$ , computed over a symmetrical temporal window of length  $\omega$ . This attribute is designed to quantify the local energy content of the seismic signal within a defined time interval and is widely used in amplitude-based seismic interpretation

### Seismic Inversion for Acoustic Impedance and Porosity

Seismic inversion translates seismic reflectivity data into quantitative rock property models. One of the principal outputs is Acoustic Impedance (AI), defined as the product of density and compressional velocity, which can be related to lithology and porosity. Theoretically, AI inversion is based on the convolutional model, where the seismic trace is assumed to result from the convolution of a source wavelet with the Earth's reflectivity series—approximated as the logarithmic derivative of AI. However, this inversion process is inherently ill-posed, being highly sensitive to vertical resolution limits, ambient seismic noise, and inaccuracies in wavelet estimation. In post-stack data, where AVO information is unavailable, the problem is further constrained, reducing the ability to resolve subtle elastic contrasts. To ensure inversion stability under these conditions, strategies such as careful wavelet extraction, low-frequency trend incorporation from well logs, and regularization through statistical or Bayesian frameworks are typically employed. These approaches help suppress spurious oscillations, compensate for lost low-frequency content, and stabilize the solution by incorporating prior geological knowledge.

$$AI = \rho \cdot V_p \quad (4)$$

The reflection coefficient  $R$  at an interface between two lithologies is given by:

$$R = \frac{AI_2 - AI_1}{AI_2 + AI_1} \quad (5)$$

AI is often used in reservoir characterization because it provides indirect sensitivity to porosity and fluid content [1]. In the context of clastic systems—sedimentary environments dominated by fragments of pre-existing rocks such as sandstones, siltstones, and shales—porosity typically exhibits an inverse correlation with AI [13]. This relationship arises because higher porosity generally implies lower rock density and velocity, leading to reduced acoustic impedance, particularly in unconsolidated or poorly cemented siliciclastic formations like those found in the F3 Block.

An empirical multilinear regression model to estimate porosity can be written as:

$$\phi = a_0 + a_1 \cdot AI + a_2 \cdot Attribute_1 + \dots + a_n \cdot Attribute_n \quad (6)$$

### Bayesian Ridge Regression (BRR)

Bayesian Ridge Regression (BRR) extends traditional linear regression by placing prior probability distributions over the model parameters, allowing for a principled balance between data fit and model complexity [4]. Using Bayes' theorem, BRR estimates the posterior distribution of the regression coefficients, which reduces the risk of overfitting and enables uncertainty quantification. The model assumes Gaussian priors on the weights and noise, and automatically determines regularization strength through evidence maximization—also known as marginal likelihood optimization. This framework not only stabilizes the solution in noisy or ill-posed settings but also supports Bayesian model comparison based on posterior evidence. The linear model is expressed as:

$$y = Xw + \varepsilon \quad (7)$$

$$\varepsilon \sim N(0, \alpha^{-1}I), \quad w \sim N(0, \lambda^{-1}I) \quad (8)$$

Equation (7) and (8) form the foundation of the Bayesian Ridge Regression (BRR) framework. Equations (7) and (8) serve as the backbone of the Bayesian Ridge Regression (BRR) paradigm. Specifically, Equation (7) delineates the target vector  $y$  as a weighted projection of the feature matrix  $X$  via the coefficient vector  $w$ , while embedding a stochastic disturbance term  $\varepsilon$  to encapsulate all chaotic or unexplained variations unaccounted for by the deterministic linear formulation.

Equation (8) introduces the probabilistic assumptions underlying BRR. It assumes that the noise  $\varepsilon$  follows a Gaussian distribution with zero mean and precision  $\alpha$  (i.e.,  $\varepsilon \sim \mathcal{N}(0, \alpha^{-1})$ ). The precision is the inverse of the variance and reflects how tightly the noise is expected to concentrate around the mean. Similarly, the weight vector  $w$  is assigned a zero-mean Gaussian prior with precision  $\lambda$  (i.e.,  $w \sim \mathcal{N}(0, \lambda^{-1}I)$ ). This prior distribution regularizes the model by discouraging large weight magnitudes, which is especially useful in cases with multicollinearity or limited training data.

Together, these two equations define a Bayesian formulation of linear regression that balances model fit and complexity. Unlike classical linear regression, which provides point estimates of coefficients, BRR estimates their full posterior distribution, enabling uncertainty quantification and robust predictions under noisy or high-dimensional settings

The posterior distribution over model weights is given as a multivariate Gaussian [14]:

$$p(w | X, y) = N(w | \mu, \Sigma) \quad (9)$$

$$\Sigma = (\alpha X^T X + \lambda I)^{-1} \quad (10)$$

$$\mu = \alpha \Sigma X^T y \quad (11)$$

This regression method is especially robust when applied to high-dimensional seismic datasets, as supported by the Scikit-learn framework documentation [15].

### Methodology

In this study, we utilized an open-access dataset from the Dutch sector of the North Sea, specifically the F3 Block, which includes a 3D post-stack seismic volume and two accompanying well logs, hereafter referred to as Well 34 and Well 61. Initial preprocessing was conducted using a 2D seismic extraction with a temporal sampling rate of 4 ms and 911 traces. The F3 Block is characterized by deltaic siliciclastic deposition with alternating sand–shale sequences, where fluid-sensitive impedance contrasts and subtle stratigraphic variations present a suitable testbed for multi-attribute inversion workflows. Due to the moderate burial depth and the presence of unconsolidated marine sediments, the seismic reflectivity in this area is expected to have a strong correspondence with acoustic impedance variations—thus making it highly relevant to employ a physics-guided inversion strategy.

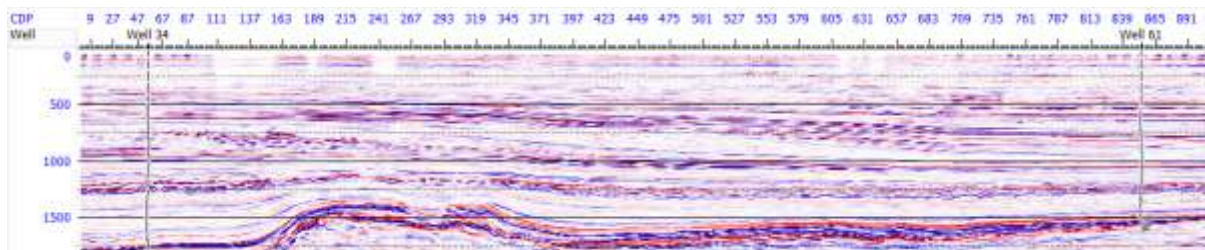


Fig 1. Position of 2 Wells in Seismic Traces

The initial phase of the methodology involved anchoring the temporal seismic domain to subsurface geological markers via a rigorous well-to-seismic alignment. This calibration entailed synthetically generating a seismic trace by convolving the reflectivity—computed from wellbore-derived velocity and density profiles—with a representative wavelet extracted from the seismic data. In this study, a statistical wavelet with a length of 100 ms was utilized to capture the average seismic response across the volume. The synthetic and observed traces were then meticulously correlated and manually realigned to ensure that seismic events accurately mirrored lithological boundaries encountered in the borehole. After alignment, the resulting time shifts at both Well 34 and Well 61 were 0 ms, indicating a successful tie with no residual misfit. The final correlation coefficients were 0.808 for Well 34 and 0.748 for Well 61, reflecting reliable temporal correspondence between seismic and geological markers. These values are considered robust, especially given the inherent limitations of post-stack data where angle-dependent effects and full waveform information are absent.

To reconcile the mismatch in sampling intervals between seismic traces (originally at 4 ms) and well logs (typically recorded at sub-millisecond resolution), the seismic data were temporally upsampled to a denser sampling grid equivalent to 2 ms spacing. The upsampling was carried out using linear interpolation over a normalized time axis, where each trace was resampled from its original discrete points to a higher-resolution grid. This method does not explicitly preserve spectral content or account for frequency-domain behavior, but it offers a computationally efficient means of increasing vertical sample density. This step is particularly important in deltaic depositional environments like the F3 Block, where thin-bedded sand–shale alternations produce subtle impedance contrasts that may be under-resolved at coarser sampling intervals.

Following the preprocessing stage, a suite of ten seismic attributes was computed from the upsampled dataset. These include: (1) raw amplitude, (2) amplitude gradient, (3) Hilbert envelope, (4) envelope derivative, (5) RMS amplitude, (6) Gaussian-filtered amplitude, (7)

relative impedance (logarithmic reflectivity), (8) instantaneous phase, (9) second-order trace curvature, and (10) smoothed amplitude using medium-scale Gaussian filtering.

These attributes were deliberately selected based on their complementary physical sensitivity. For instance, the envelope and RMS amplitude highlight signal energy and reflector continuity; curvature and phase accentuate stratigraphic geometry; while log reflectivity and gradient-based attributes are direct proxies for lithological contrasts. In the context of the F3 Block, such diversity is crucial to capture both structural deformation and depositional variability, especially across channelized sand lobes and interbedded shales.

To infer subsurface rock properties from these seismic attributes, we implemented a multi-attribute inversion framework based on Bayesian Ridge Regression (BRR). This statistical approach is particularly suited for ill-posed geophysical inversion problems where multicollinearity among predictors is prevalent. BRR introduces regularization via Gaussian priors over the model weights, stabilizing the solution and providing not only point estimates but also posterior uncertainty. The inversion was carried out in two stages: First, the model was trained independently for each well using time-aligned intervals between seismic and log-derived acoustic impedance and porosity. Second, the trained models were applied trace-by-trace across the seismic volume to generate spatial predictions.

The expected outcome of this methodology is the generation of detailed 2D property maps that maintain lateral continuity, vertical geological resolution, and consistency with available well data. Specifically, the acoustic impedance and porosity maps are expected to reveal lateral variations corresponding to deltaic lobes, channel-fill systems, and potentially hydrocarbon-charged reservoirs. The incorporation of ten diverse seismic attributes allows the inversion to detect complex lithological changes and subtle transitions in depositional facies that may not be apparent in single-attribute analysis. The overall workflow is summarized in Fig. 2. Below:

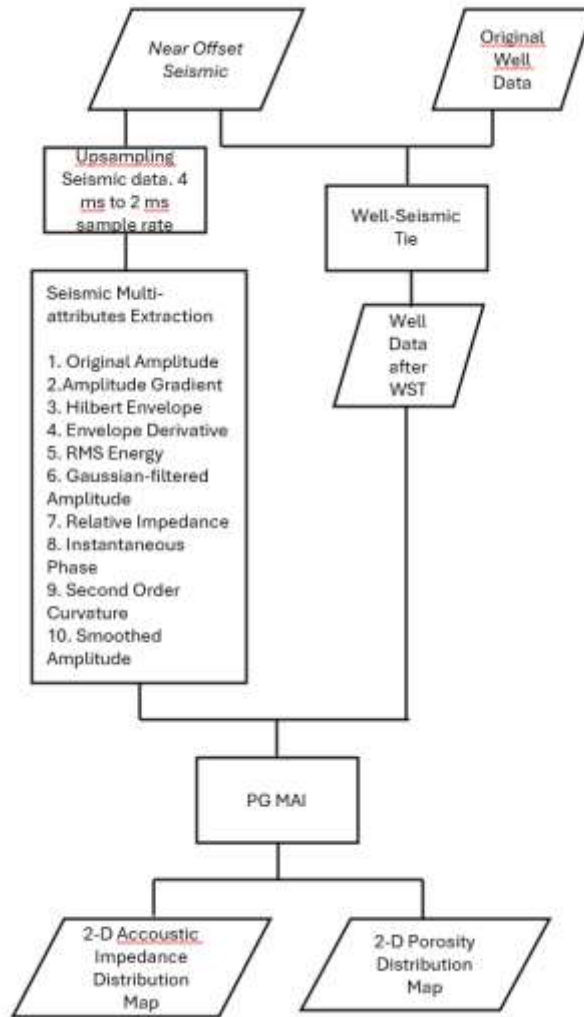


Fig 2. PG MAI Workflow

## RESULTS AND DISCUSSION

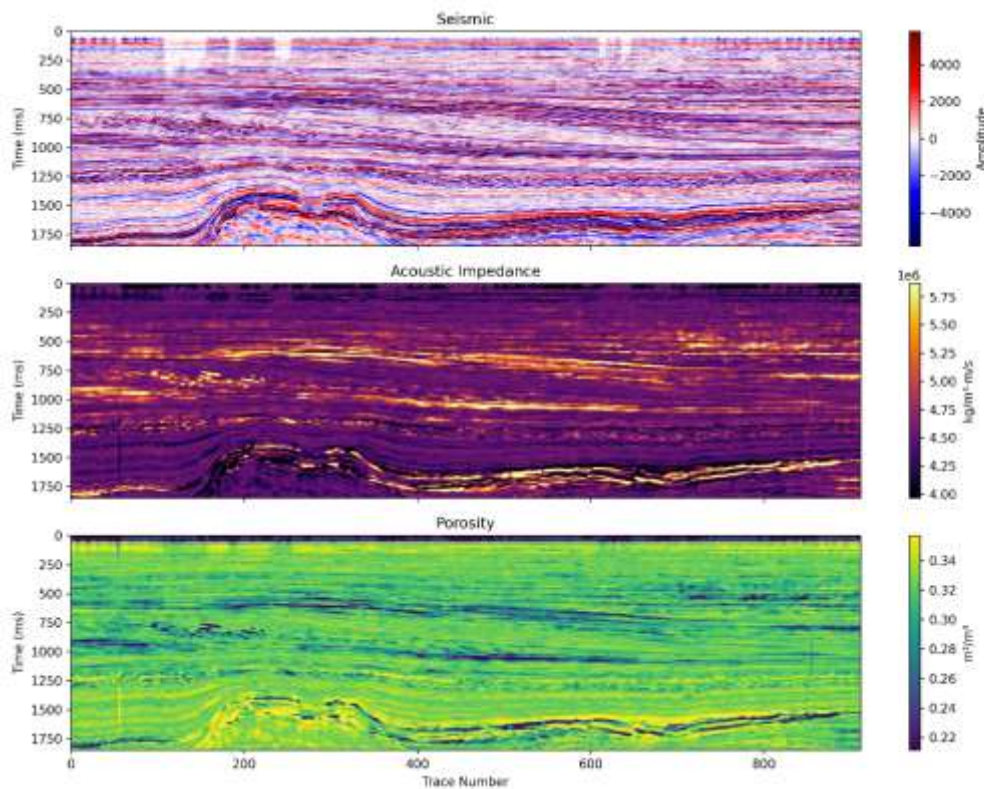


Fig 3. 2-D Distribution of Acoustic Impedance and Porosity

Fig. 3 presents the two-dimensional spatial distribution of both acoustic impedance (AI) and porosity derived from the PG-MAI inversion workflow. The AI distribution displays clear lateral variability, which corresponds to the interpreted stratigraphic sequences in the F3 Block. Low AI values, ranging from approximately  $2.5 \times 10^6$  to  $3.5 \times 10^6$   $\text{kg/m}^3 \cdot \text{m/s}$ , appear in horizontally continuous bands that are interpreted as unconsolidated, sand-rich layers with high porosity. These values are in agreement with prior inversion studies applied to the F3 Block that report comparable ranges of AI in similar depositional facies [16]. In contrast, higher AI values exceeding  $4.5 \times 10^6$   $\text{kg/m}^3 \cdot \text{m/s}$  are associated with compacted shale intervals, which exhibit lower porosity and higher acoustic velocities, as also reported in other studies on deltaic sequences [17].

From a stratigraphic perspective, the lateral continuity and the alternation of impedance contrasts reflect the stacking of delta-front parasequences. These parasequences likely preserve coarsening- or fining-upward cycles that are expressed as seismic-scale impedance layering. The observed alternating high–low AI patterns may indicate shifts between distributary mouth bars and interdistributary bays. In sections between trace numbers 200–400 and 600–850, subtle terminations and undulations in AI values could correspond to channel truncations or lobe boundary contacts, which are common in deltaic systems. However, these interpretations remain preliminary and would benefit from further validation through seismic facies classification and detailed horizon-based stratigraphic correlation. Such future work is essential to strengthen the geological framework and confirm the depositional significance of the observed impedance patterns.

The porosity distribution in Fig. 3 reveals zones exceeding 30% porosity, particularly in shallower intervals, consistent with previous findings that identified clean sands with excellent reservoir quality in this field. These patterns reflect the alternation of high-energy sand-prone facies and low-energy shale-dominated layers, characteristic of a delta-front depositional environment. The match between low-AI zones and high-porosity values supports the geological consistency of the inversion. These features also suggest facies transitions from proximal deltaic sands to more distal shale-prone environments.

In addition, the vertical stacking of high-porosity zones with lateral extension indicates the presence of stratigraphically controlled reservoirs. This implies that the PG-MAI inversion is capable of capturing not just lithological variation, but also depositional architecture. The lateral continuity of both AI and porosity features supports the geological plausibility of the inversion output and underscores the method's robustness in resolving stratigraphic variations.

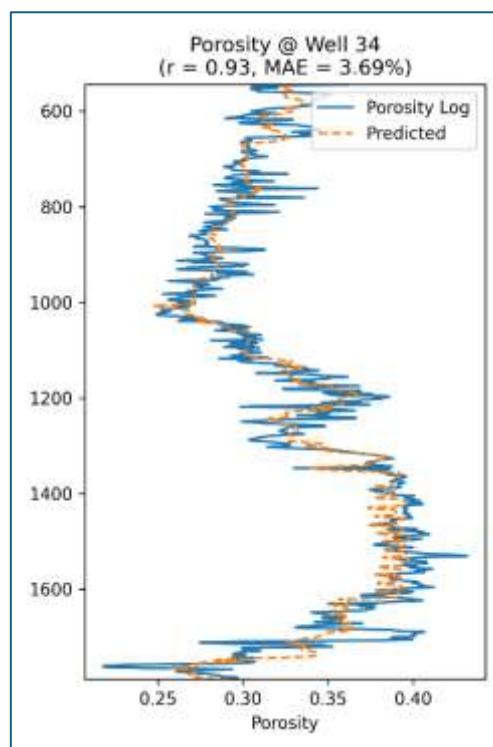


Fig 4. Porosity log vs Predicted Porosity of Well 34

The comparison between predicted and logged porosity in Well 34, as shown in Fig. 4, indicates a strong correlation of 0.93. The predicted log effectively captures variations across the stratigraphic interval dominated by delta-front sandstones. This agreement confirms the predictive power of the PG-MAI framework in handling subtle waveform variations related to sedimentary transitions in post-stack seismic data [3]. The porosity profile reflects the geological alternation between sand-prone and shale-prone sequences within the F3 Block's shallow marine depositional system, a pattern well-documented in North Sea analogs [8]. The effectiveness of the Bayesian Ridge approach in this case lies in its ability to generalize from limited well data while preserving vertical resolution, even in zones with weaker reflectivity contrasts [4].

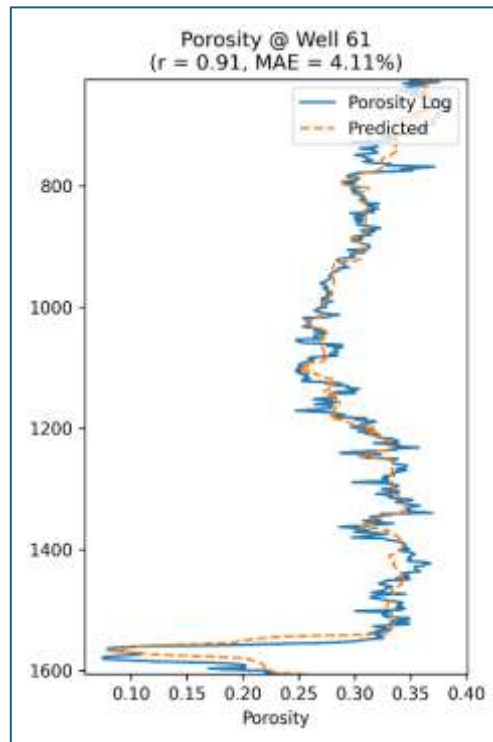


Fig 5. Porosity log vs Predicted Porosity of Well 61

Fig. 5 displays the porosity prediction for Well 61, where a similarly high correlation coefficient of 0.91 is achieved. The model demonstrates robust alignment across both shallow and intermediate intervals, reinforcing the spatial consistency of attribute-porosity relationships across wells. Given the lateral facies heterogeneity typical of the F3 Block's deltaic depositional setting, this level of predictive performance is significant and confirms the stability of the inversion method [10]. The strong agreement across both wells suggests that the selected seismic attributes—especially the envelope, RMS, and log-impedance ratio—carry meaningful geological information tied to porosity-bearing units [1]. This supports prior findings that multi-attribute methods are particularly suitable in environments with complex lithological transitions [5].

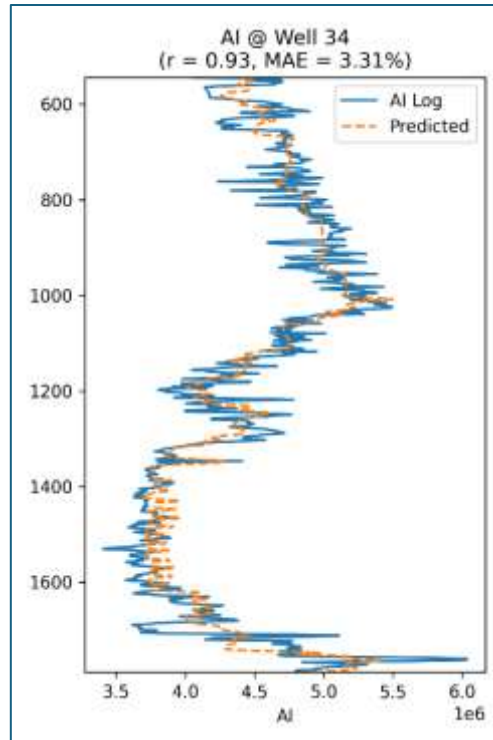


Fig 6. AI vs Predicted AI of Well 34

Figure 6 presents the comparison between the actual and predicted acoustic impedance (AI) log at Well 34. The overall correlation coefficient is 0.93, reflecting strong agreement across the stratigraphic section. The predicted AI closely follows the trend of the measured log, where transitions between sand and shale dominate. This accuracy can be attributed to the sensitivity of attributes like Hilbert envelope, log-impedance ratio, and RMS amplitude in capturing changes in reflectivity tied to lithological interfaces [3].

In deltaic environments such as the F3 Block, AI serves as a proxy for lithological variation, where lower impedance typically corresponds to porous sandstones and higher impedance indicates compacted shale [1]. The ability of the PG-MAI method to detect such transitions implies that the multi-attribute set effectively resolves acoustic contrasts, even under the limited vertical resolution of post-stack data. Similar studies in clastic successions have shown that multi-attribute inversion using BRR improves model generalization and reduces susceptibility to local noise [4]. The results also align with known rock physics trends where acoustic impedance inversely correlates with porosity in unconsolidated siliciclastic formations [10].

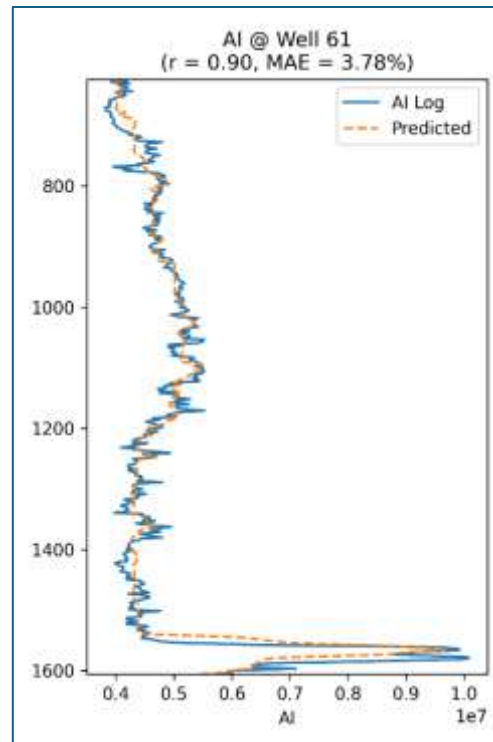


Fig 7. AI vs Predicted AI of Well 61

Figure 7 shows the predicted acoustic impedance (AI) for Well 61, which exhibits a strong match with the measured log, supported by a high correlation coefficient of 0.91. This result demonstrates that the PG-MAI framework effectively captures the lateral and vertical acoustic contrasts resulting from lithological variations in the F3 Block [3]. The use of envelope, relative impedance, curvature, and other derived attributes significantly enhances the inversion sensitivity to reflection geometry and stratigraphic architecture [10]. These results reflect the interbedded nature of deltaic sandstone and shale deposits in the study area, where impedance changes arise due to porosity contrasts and sedimentary heterogeneity [5]. Overall, implementation of the PG-MAI inversion method demonstrates a significant enhancement in predicting subsurface petrophysical properties from post-stack seismic data. By integrating a diverse suite of seismic attributes—sensitive to amplitude, phase, and frequency content—the method effectively compensates for the absence of angle variation in post-stack gathers. This approach improves lateral continuity and the vertical resolution of inverted properties, consistent with previous findings that emphasize the value of attribute complementarity for inversion performance [10]. In the context of the F3 Block, this is particularly relevant given its complex depositional environment, where distinguishing subtle variations in lithology and stratification is critical for delineating reservoir zones.

Well-log correlations exceeding 0.90 in both porosity and acoustic impedance predictions validate the model's robustness in capturing petrophysical trends with minimal deviation from ground truth data. The stratigraphy of the F3 Block is characterized by alternating sand-shale sequences deposited in a shallow marine deltaic system, where high-energy sandstone lobes are interbedded with lower-energy muddy layers. This facies architecture requires inversion techniques capable of detecting abrupt impedance contrasts and subtle porosity variations

across stratigraphic boundaries. The PG-MAI method shows competence in tracing these transitions, thereby enabling improved reservoir delineation and facies prediction.

Furthermore, the application of Bayesian Ridge Regression provides an effective balance between fitting the seismic-derived attributes and generalizing beyond noise artifacts. Its regularization properties are essential in inversion domains where data density is spatially uneven or well control is sparse—conditions commonly encountered in mature offshore settings [17]. The resulting impedance and porosity models honor the regional geological understanding of the F3 Block, reflecting the progradational patterns and compaction trends typical of North Sea clastic systems.

Accurate mapping of acoustic impedance and porosity plays a pivotal role in guiding drilling decisions and reservoir development strategies. Seismic inversion, particularly when enhanced with multi-attribute frameworks, has demonstrated the ability to reduce uncertainty in lithological interpretation and improve the delineation of prospective zones. This is especially critical in stratified clastic environments where facies transitions occur over short vertical and lateral distances. Several studies have emphasized that the integration of inversion-derived properties with petrophysical trends enhances the reliability of static reservoir models, while simultaneously minimizing the risk of misinterpretation caused by amplitude ambiguities or noise artifacts [18].

Moreover, the use of acoustic impedance inversion in combination with attribute analysis has proven effective in capturing porosity variations across channelized sand bodies and interbedded sequences, which are often difficult to resolve using conventional amplitude-based interpretation. Such inversion strategies contribute directly to identifying reservoir sweet spots, estimating effective thickness, and refining volumetric calculations [19]. These capabilities underscore the strategic importance of physics-guided inversion approaches—like PG-MAI—in maximizing predictive accuracy and operational efficiency in data-constrained exploration settings.

## **CONCLUSION AND RECOMMENDATION**

### **Conclusion**

This study presented the implementation of a Physics-Guided Multi-Attribute Inversion (PG-MAI) framework that combines Bayesian Ridge Regression with a physically interpretable and statistically validated set of seismic attributes to estimate acoustic impedance (AI) and porosity from post-stack seismic data. The method was applied to the F3 Block, a stratigraphically complex marine-deltaic reservoir characterized by interbedded sandstone and shale sequences. This setting provided a suitable test case for inversion under conditions of lithological heterogeneity and limited well control. The PG-MAI framework delivered strong predictive performance, with correlation coefficients exceeding 0.90 at two well locations. The inversion outcomes reflected both lateral and vertical continuity, capturing geological features that align with expected depositional architectures, such as deltaic lobes and parasequence stacking. These results affirm the model's capability to resolve geologically significant heterogeneities, even when working with the limited bandwidth and resolution constraints of post-stack seismic data.

Beyond predictive accuracy, the PG-MAI approach contributes to the advancement of seismic inversion methodologies by addressing key limitations present in both conventional and data-driven techniques. Unlike standard linear inversions, which often fail to account for lithological variability and struggle in underconstrained regions, PG-MAI introduces regularization through Bayesian priors, thereby enhancing model robustness while retaining transparency in parameter estimation. Compared to black-box machine learning models such as support vector regression or deep neural networks, PG-MAI remains interpretable, reproducible, and physically grounded, making it more suitable for geological workflows that require traceability of assumptions and outputs. The use of Bayesian Ridge Regression further allows for automatic control over model complexity, reducing the risk of overfitting without the need for exhaustive hyperparameter tuning. This balance of physical constraints and statistical flexibility makes the framework particularly well-suited for applications where well calibration is sparse and geological uncertainty is high.

The selection of seismic attributes was a crucial step in improving inversion reliability. Instead of relying on ad hoc or exhaustive feature inclusion, ten attributes were selected based on a combination of domain knowledge, sensitivity to lithological variation, and statistical relevance to the target properties. These included amplitude-based features (e.g., RMS energy, envelope), geometrical descriptors (e.g., curvature, gradient), and phase-related components (e.g., instantaneous phase), along with attributes such as relative impedance and smoothed reflectivity that were designed to approximate rock-physics behavior. Redundancy among attributes was reduced through correlation filtering to ensure that each input contributed unique information. This curated set of features enabled the model to capture subtle depositional variations and stratigraphic transitions that are often obscured in conventional single-attribute inversions. In conclusion, the PG-MAI framework presents a geologically consistent, physically informed, and statistically optimized approach to seismic inversion, offering a valuable tool for improving reservoir delineation, fluid prediction, and subsurface characterization in complex siliciclastic systems.

## **Recommendation**

To improve the efficiency and reproducibility of the PG-MAI workflow in future applications, particularly in data-constrained environments similar to this study, several targeted recommendations are proposed:

- a. Future work should evaluate different window sizes systematically, potentially using geological or stratigraphic intervals as guidance, to fine-tune vertical resolution
- b. The ten attributes used in this study were selected based on prior interpretability, but in future implementations, applying a variance inflation factor (VIF) or correlation matrix analysis could help avoid overlapping or redundant predictors, which may degrade model robustness.
- c. Although well logs provide reliable calibration, additional validation against core-derived porosity or production performance (e.g., flow zones, water breakthrough) would further enhance model confidence and bridge static-dynamic integration.

## REFERENCES

- [1] P. Avseth, T. Mukerji, and G. Mavko, *Quantitative Seismic Interpretation: Applying Rock Physics Tools to Reduce Interpretation Risk*. Cambridge: Cambridge University Press, 2005.
- [2] B. Russell and D. Hampson, "Comparison of post-stack seismic inversion methods," *CSEG Recorder*, vol. 16, no. 7, pp. 23–28, 1991.
- [3] D. Hampson, J. Schuelke, and J. Quirein, "Use of multi-attribute transforms to predict log properties from seismic data," *Geophysics*, vol. 66, no. 1, pp. 220–236, 2001, doi: [10.1190/1.1444899](https://doi.org/10.1190/1.1444899).
- [4] M. E. Tipping, "Sparse Bayesian learning and the relevance vector machine," *Journal of Machine Learning Research*, vol. 1, pp. 211–244, 2001.
- [5] H. Wu, "Deterministic and Stochastic Inversion Techniques Used to Predict Porosity: A Case Study from F3-Block", M.S. thesis, Michigan Technological University, 2015.
- [6] A. S. van der Molen and W. Börner, "Lower Cretaceous of the Southern North Sea Basins: Reservoir distribution within a sequence stratigraphic framework," ResearchGate, 2015. [Online]. Available: <https://www.researchgate.net/publication/288272163>
- [7] R. Ravnås, S. Curcic, and K. E. Bang-Kittilsen, "Sequence stratigraphy of the Jurassic–Lowermost Cretaceous (Hettangian–Berriasian) of the North Sea Region," *Geological Society of London, Memoir*, vol. 59, 2024.
- [8] L. Adeoti *et al.*, "Porosity prediction using 3D seismic genetic inversion at F3 Block, Offshore Netherlands," *Ife Journal of Science*, vol. 25, no. 1, pp. 69–81, 2023.
- [9] N. P. Singh, "Porosity prediction from offshore seismic data of F3 Block, the Netherlands using MLFN," *Current Science*, vol. 119, no. 9, pp. 1484–1491, 2020.
- [10] S. Chopra and K. J. Marfurt, *Seismic Attributes for Prospect Identification and Reservoir Characterization*. Tulsa, OK, USA: Soc. Expl. Geophysicists, 2007.
- [11] M. T. Taner, F. Koehler, and R. E. Sheriff, "Complex seismic trace analysis," *Geophysics*, vol. 44, no. 6, pp. 1041–1063, 1979, doi: [10.1190/1.1440994](https://doi.org/10.1190/1.1440994).
- [12] M. T. Taner, "Seismic attributes," *CSEG Recorder*, vol. 26, no. 6, pp. 48–56, 2001.
- [13] J. L. Mari and F. Glangeaud, "Inversion of seismic data and well logs for porosity estimation," *Oil & Gas Science and Technology – Rev. IFP*, vol. 61, no. 4, pp. 483–494, 2006.
- [14] C. M. Bishop, *Pattern Recognition and Machine Learning*. New York, NY, USA: Microsoft, 2006.
- [15] F. Pedregosa *et al.*, "Scikit-learn: Machine learning in Python," *J. Mach. Learn. Res.*, vol. 12, pp. 2825–2830, 2011.
- [16] P. K. Kushwaha, Richa, S. P. Maurya, P. Rai, and N. P. Singh, "Comparison of Band-limited and Colored Seismic Inversion Methods to Estimate Acoustic Impedance of F3 Block Netherlands – A Case Study," in *SPG India Conference*, 2020.

- [17] T. Mukerji and D. Grana, "Bayesian methods applied to rock physics and reservoir characterization," in *Quantitative Seismic Interpretation*. Society of Exploration Geophysicists, 2015.
- [18] E. S. Nugroho, A. Riyanto, and M. Suardana, "Reservoir characterization with acoustic impedance inversion and multi-attribute method," *IOP Conf. Ser.: Mater. Sci. Eng.*, vol. 854, no. 1, p. 012063, 2020.
- [19] M. S. Siregar, "Statistical tuning chart for mapping porosity thickness: A case study of channel sand bodies," *Proc. 42nd Indonesian Petroleum Association Annual Convention and Exhibition*, 2018.